ITRF2000 JGR Publication

The permisson to reprint the publication

Altamimi, Z., P. Sillard, and C. Boucher, ITRF2000: A new release of the International Terrestrial Reference Frame for earth science applications, *J. Geophys. Res.*, *107*(B10), 2214, doi:10.1029/2001JB000561, 2002.

as part of the IERS Technical Note No. 31 has been granted to the IERS by the AGU. The article is copyright by the American Geophysical Union and appears without modification.

ITRF2000: A new release of the International Terrestrial Reference Frame for earth science applications

Zuheir Altamimi, Patrick Sillard, and Claude Boucher[1]
Institut Géographique National, Paris, France

Received 7 May 2001; revised 15 March 2002; accepted 20 March 2002; published 8 October 2002.

[1] For the first time in the history of the International Terrestrial Reference Frame, the ITRF2000 combines unconstrained space geodesy solutions that are free from any tectonic plate motion model. Minimum constraints are applied to these solutions solely in order to define the underlying terrestrial reference frame (TRF). The ITRF2000 origin is defined by the Earth center of mass sensed by satellite laser ranging (SLR) and its scale by SLR and very long baseline interferometry. Its orientation is aligned to the ITRF97 at epoch 1997.0, and its orientation time evolution follows, conventionally, that of the no-net-rotation NNR-NUVEL-1A model. The ITRF2000 orientation and its rate are implemented using a consistent geodetic method, anchored over a selection of ITRF sites of high geodetic quality, ensuring a datum definition at the 1 mm level. This new frame is the most extensive and accurate one ever developed, containing about 800 stations located at about 500 sites, with better distribution over the globe compared to past ITRF versions but still with more site concentration in western Europe and North America. About 50% of station positions are determined to better than 1 cm, and about 100 sites have their velocity estimated to at (or better than) 1 mm/yr level. The ITRF2000 velocity field was used to estimate relative rotation poles for six major tectonic plates that are independent of the TRF orientation rate. A comparison to relative rotation poles of the NUVEL-1A plate motion model shows vector differences ranging between 0.03° and 0.08°/m.y. (equivalent to approximately 1–7 mm/yr over the Earth's surface). ITRF2000 angular velocities for four plates, relative to the Pacific plate, appear to be faster than those predicted by the NUVEL-1A model. The two most populated plates in terms of space geodetic sites, North America and Eurasia, exhibit a relative Euler rotation pole of about 0.056 (±0.005)°/m.y. faster than the pole predicted by NUVEL-1A and located about (10°N, 7°E) more to the northwest, compared to that model. *INDEX TERMS:* 1709 History of Geophysics: Geodesy; 8155 Tectonophysics: Plate motions—general; 1229 Geodesy and Gravity: Reference systems; 1247 Geodesy and Gravity: Terrestrial reference systems; *KEYWORDS:* reference systems and frames, terrestrial reference systems and frames, tectonic plate motion, ITRF

Citation: Altamimi, Z., P. Sillard, and C. Boucher, ITRF2000: A new release of the International Terrestrial Reference Frame for earth science applications, *J. Geophys. Res.*, *107*(B10), 2214, doi:10.1029/2001JB000561, 2002.

1. Introduction

[2] One of the ultimate goals of space geodesy is to estimate point positions on the Earth surface as accurately as possible. Meanwhile, point positions are neither observable nor absolute quantities and then have to be determined with respect to some reference. We refer to "terrestrial reference system" (TRS) as the mathematical object satisfying an ideal definition and in which point positions will be expressed. Nevertheless, the access to point positions requires some observational means allowing their link to the mathematical object. We therefore call a "terrestrial reference frame" (TRF), a physical materialization of the TRS, making use of observations derived from space geodesy techniques.

[3] The distinction between "system" and "frame" is then subtle since the former is rather invariable and inaccessible while the latter is accessible and perfectible. The general concepts of reference systems and frames have been extensively discussed in the 1980s within the astronomical and geodetic communities [*Kovalevsky et al.*, 1989]. They are largely described by *Boucher* [2000]. The use of space geodesy techniques since the 1980s has deeply improved positioning over the Earth's surface: The uncertainties initially of decimetric level are now of centimetric, even millimetric level.

[4] Nevertheless, each technique and each data analysis define and realize its own TRS. Therefore a multitude of TRF could exist, having systematic differences and bias

[1]Also at Ministère de la Recherche, Paris, France.

Copyright 2002 by the American Geophysical Union.
0148-0227/02/2001JB000561$09.00

when one is compared to another. This fact led the International Union of Geodesy and Geophysics (IUGG) and the International Association of Geodesy (IAG) to adopt a unique TRS, called the International Terrestrial Reference System (ITRS) for all Earth science applications [*Geodesist's Handbook*, 1992]. For the general description of the ITRS, see *McCarthy* [1996]. The ITRS origin is defined by the center of mass of the whole Earth, including oceans and the atmosphere. Its unit of length is the meter (SI) so that this scale is consistent with the geocentric coordinate time (TCG), in agreement with IAU/IUGG resolutions (1991), see the appendix of *McCarthy* [1992]. The use of TCG ensures that all physical quantities take the same value in the terrestrial coordinate system as in the barycentric system (or in any other planetocentric system). The mean rate of the coordinate time TCG coincides with the mean rate of the proper time of an observer situated at the geocenter (with the Earth removed), whereas the mean rate of the terrestrial time (TT) coincides with the mean rate of the proper time of an observer situated on the geoid [*Petit*, 2000]. The two timescales differ in rate by ($TCG - TT \approx 0.7 \times 10^{-9}$). Its orientation is consistent with that of the Bureau International de l'Heure (BIH) at 1984.0. Its orientation time evolution is ensured by a no-net-rotation condition with regards to horizontal tectonic motions over the whole Earth.

[5] The basic idea of ITRF is to combine station positions (and velocities) computed by various analysis centers, using observations of space geodesy techniques, such as very long baseline interferometry (VLBI), lunar and satellite laser ranging (LLR and SLR), Global Positioning System (GPS), and Doppler Orbitography Radiopositionning Integrated by Satellite (DORIS). The combination method has proved its efficiency to produce a global reference frame which benefits from the strengths of all these different techniques.

[6] The history of ITRF goes back to 1984, when for the first time a combined TRF (called BTS84), was established using station coordinates derived from VLBI, LLR, SLR, and Doppler/TRANSIT (the predecessor of GPS) observations [*Boucher and Altamimi*, 1985]. BTS84 was realized in the framework of the activities of BIH, being a coordinating center for the international project called Monitoring of Earth Rotation and Intercomparison of Techniques (MERIT) [*Wilkins*, 1989]. Three other successive BTS realizations were then achieved, ending with BTS87 [see *Observatoire de Paris*, 1986, 1987, 1988], when in 1988, the IERS was created by the IUGG and the International Astronomical Union (IAU).

[7] Since the first ITRS realization, namely, ITRF88, eight other ITRF versions were established and published, each of which superseded and replaced its predecessor. Substantial improvements have since been constantly made in the data analysis strategy to achieve optimal combination for ITRF generation [*Altamimi et al.*, 1993; *Boucher and Altamimi*, 1993, 1996; *Sillard et al.*, 1998].

[8] As the ITRF solutions are widely used in geodetic and geophysical applications, the ITRF2000 is intended to be an improved frame in terms of quality, network and datum definition. The ITRF2000 solution reflects the actual quality of space geodesy solutions, being free from any external constraints. It includes primary core stations observed by VLBI, LLR, SLR, GPS, and DORIS (usually used in previous ITRF versions) as well as regional GPS networks for its densification. To ensure its time evolution stability, the ITRF2000 orientation rate has been implemented on a selection of high quality geodetic sites. (All ITRF2000 results and related files are available at http://lareg.ensg.ign.fr/ITRF/ITRF2000.)

2. ITRF2000 Input Data

2.1. Space Geodesy Solutions

[9] In order to facilitate the exchange of space geodesy results between analysis centers and research groups, a well-documented and flexible format was necessary. A working group was formed in 1994 by the International GPS Service (IGS), involving ITRF section, to establish such a format. The SINEX acronym (Software Independent Exchange) was suggested by *Blewitt et al.* [1994], and the first versions, 0.04, 0.05, and 1.00 evolved from the work and contributions of the SINEX Working Group chaired by G. Blewitt. The SINEX format was then born and widely used by all IGS and IERS analysis centers. SINEX format, by its structure, is designed to contain estimated parameters such as station positions, velocities, Earth orientation parameters, and estimated and a priori (constraint) matrices.

[10] From the beginning of the ITRF2000 project, the IERS analysis centers were encouraged and assisted to provide TRF solutions without any external constraint that would disturb their results. The rationale behind this goal is to try to assess the real quality of station positions and velocities provided by space geodesy techniques. The submitted geodetic solutions incorporated in the ITRF2000 combination are of three types, according to the initial constraints applied upon all or a subset of stations: (1) removable constraints, solutions for which the estimated station positions/velocities are constrained to external values within an uncertainty $\sigma \approx 10^{-5}$ m for positions and m/yr for velocities; this type of constraints is easily removable as described in Appendix A; (2) loose constraints, solutions where the uncertainty applied to the constraints is $\sigma \geq 1$ m for positions and $\geq$10 cm/yr for velocities; and (3) minimum constraints used solely to define the TRF using a minimum amount of required information, in a similar approach to the one described in Appendix A.

[11] These solutions are basically station positions and velocities with full variance matrices provided in SINEX format. These data are listed in Table 1, where for each solution the type of constraints, loose, removable, or minimum, is indicated. Observations used in these solutions span about 20 years for pioneering space geodesy techniques (LLR, VLBI, SLR) and approximately 10 years for GPS and DORIS techniques.

2.2. Local Surveys in Collocation Sites

[12] When combining TRF solutions provided by different techniques, it is essential to have sufficient collocation sites. A collocation site is defined by the fact that two or more space geodesy instruments are occupying simultaneously or subsequently very close locations which are very precisely surveyed in three dimensions, using classical surveys or the GPS technique. Classical surveys are usually direction angles, distances, and spirit leveling measurements between instrument reference points or geodetic markers. Adjustments of local surveys are performed by national

Table 1. Individual TRF Solutions Used in the ITRF2000 Combination

Analysis Center (AC)	AC TRF	Data Span	Stn.[a]	C[b]	σ_s[c]	σ_s[d]
VLBI						
Geodetic Institute of Bonn University (GIUB)	00 R 01	84–99	51	L	3.718	3.663
Goddard Space Flight Center (GSFC)	00 R 01	79–99	130	L	2.558	1.684
Shanghai Astronomical Observatory (SHA)	00 R 01	79–99	127	L	2.372	1.742
LLR						
Forschungseinrichtung Satellitengeodaesie (FSG)	00 M 01	77–00	3	L	2.979	
SLR						
Australian Surveying and Land Information Group (AUS)	00 L 01	92–00	55	L	0.056	0.057
Centro Geodesia Spaziale, Matera (CGS)	00 L 01	84–99	94	L	5.576	5.506
Communications Research Laboratory (CRL)	00 L 02	90–00	60	L	2.748	2.521
Center for Space Research (CSR)	00 L 04	76–00	139	L	3.098	2.798
Delft Ins. Earth Oriented Space Research (DEOS)	00 L 01	83–99	91	L	7.026	6.193
Deutsches Geodädtisches Forschungsinstitut (DGFI)	00 L 01	90–00	43	R	15.393	13.690
Joint Center for Earth System Technology, GSFC (JCET)	00 L 05	93–00	48	L	8.103	8.165
GPS						
Center for Orbit Determination in Europe (CODE)	00 P 03	93–00	160	M	78.088	65.852
GeoForschungsZentrum Potsdam (GFZ)	00 P 01	93–00	98	M	0.328	0.304
International GPS Service by Natural Resources Canada (IGS)	00 P 46	96–00	179	M	1.095	0.921
Jet Propulsion Laboratory (JPL)	00 P 01	91–99	112	M	8.847	7.663
Univ of Newcastle upon Tyne (NCL)	00 P 01	95–99	90	M	3.392	3.222
NOAA, National Geodetic Survey (NOAA)	00 P 01	94–00	165	R	58.908	56.640
DORIS						
Groupe de Recherche de Geodesie Spatiale (GRGS)	00 D 01	93–00	66	L	3.498	3.517
Institut Géographique National (IGN)	00 D 09	92–00	80	M	10.384	10.507
Multitechnique						
GRIM5 (GRGS+GFZ): SLR + DORIS + PRARE (GRIM)	00 C 01	85–99	183	L	1.418	1.841
CSR: SLR + DORIS on TOPEX (CSR)	00 C 01	93–00	147	L	4.409	4.119
GPS densification						
CORS Network by NOAA (CORS)	00 P 01	94–99	80	R	57.233	48.287
South America network by Deutsches Geodädtisches Forschungsinstitut (DGFI)	00 P 01	96–00	31	L	116.539	122.005
IAG Subcommission for Europe (EUREF) by Bundesamt für Kartographie und Geodaesie (EUR)	00 P 03	96–00	81	M	9.608	8.607
Geophysical Institute, University of Alaska (GIA)	00 P 01	96–99	20	M	6.412	6.450
Institut Géographique National (IGN)	00 P 01	98–00	28	M	4.677	4.705
Antartica network by Institut Géographique National (IGN)	00 P 02	95–00	17	M	4.266	4.058
Jet Propulsion Laboratory (JPL)	00 P 02	91–99	28	M	14.928	12.856
REGAL Network, France (REGAL)	00 P 03	96–00	29	M	10.131	8.943
Antarctica SCAR network by Institut für Planetare Geodaesie, TU Dresden (SCAR)	00 P 02	95–99	66	R	89.690	84.192

[a] Number of stations in each solution.
[b] Type of constraints applied by the individual analysis centers: L, loose; R, removable; M, minimum.
[c] The σ_s^1 is the square root of the estimated variance factor (see equation (A16)) resulting from the ITRF2000 combination.
[d] The σ_s^2 is the square root of the estimated variance factor resulting from the per-technique combinations.

geodetic agencies operating space geodesy instruments to provide differential coordinates (local ties) connecting the collocated instruments.

[13] Collocation sites represent a key element of the ITRF combination, connecting the individual TRF networks together. In addition to space geodesy solutions listed in Table 1, local ties between collocated stations are introduced in the combination with proper variances. They were collected since the beginning of ITRF activities from different sources; see, for instance, *Boucher et al.* [1999].

[14] The procedure adopted for ITRF2000 combination is to include local ties as independent solutions per site with full variance matrices using SINEX format. Unfortunately, local tie SINEX files were submitted to ITRF section by only one group, e.g., The Australian Surveying and Land Information Group (AUSLIG) for all the Australian collocation sites. Consequently, the other local ties used in the ITRF2000 combination were first converted into a complete set of positions for each site, provided in SINEX format. This has been achieved by solving for the following system of observation equations:

$$\begin{pmatrix} \Delta x_s^{i,j} \\ \Delta y_s^{i,j} \\ \Delta z_s^{i,j} \end{pmatrix} = \begin{pmatrix} x^j - x^i \\ y^j - y^i \\ z^j - z^i \end{pmatrix}, \quad (1)$$

where $(\Delta x_s^{i,j}, \Delta y_s^{i,j}, \Delta z_s^{i,j})$ are the geocentric components of the tie vector linking two points i and j, of a given data set s. The standard deviations (SD) $(\sigma\Delta x_s^{i,j}, \sigma\Delta y_s^{i,j}, \sigma\Delta z_s^{i,j})$ for each local tie vector are used to compute a diagonal variance matrix. If these SD are not available, they are computed by

$$\sigma_{\text{computed}} = \sqrt{\sigma_1^2 + \sigma_2^2}, \quad (2)$$

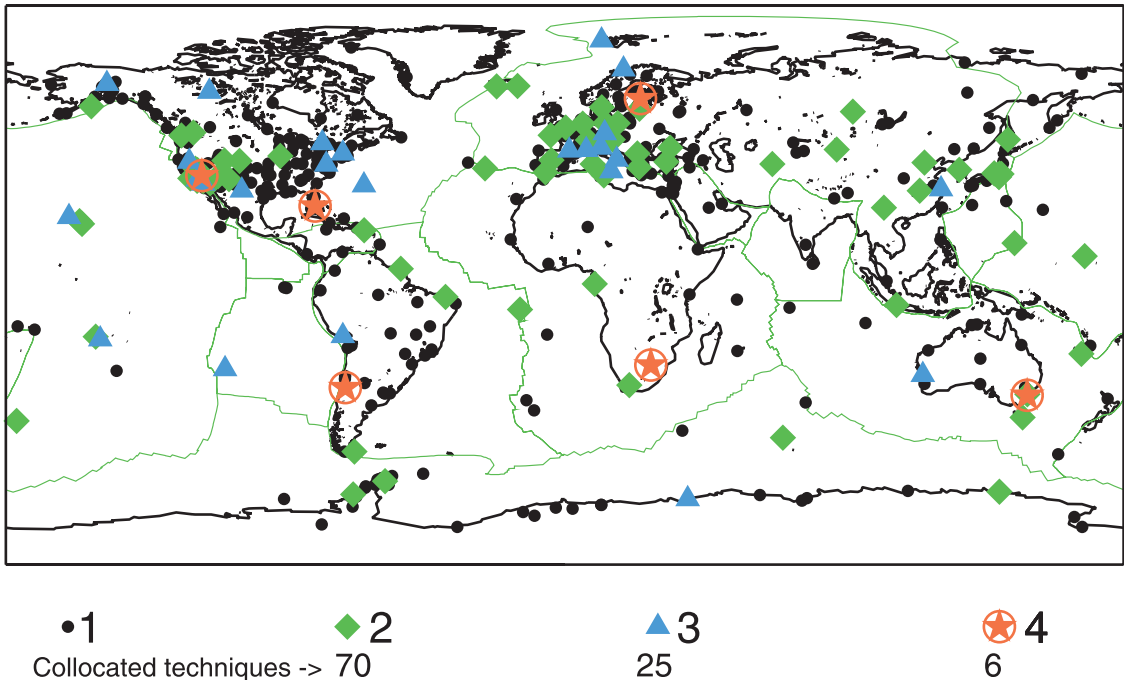

Figure 1. ITRF2000 Network and number of sites with collocated techniques.

where $\sigma_1 = 3$ mm and

$$\sigma_2 = 10^{-6} \times \sqrt{(\Delta x_s^{i,j})^2 + (\Delta y_s^{i,j})^2 + (\Delta z_s^{i,j})^2}$$

The equation system (1) needs, of course, initial coordinates for one point per tie vector set s, which are taken from ITRF solutions. Figure 1 shows the coverage of the ITRF2000 network, highlighting the sites with collocated techniques.

3. ITRF2000 Data Analysis

[15] Major innovations are implemented to enhance and to improve the ITRF2000 combined solution, e.g., (1) unconstrained individual solutions are used and to which minimim constraints are added in order to accurately define the underlying TRF in origin, scale, orientation and time evolution; (2) the ITRF2000 origin is defined by the center of mass as sensed by SLR; and (3) in order to achieve better definition of its orientation time evolution, this latter is established upon a selection of sites of high geodetic quality.

[16] The ITRF2000 analysis strategy is a collection of procedures and algorithms implemented in CATREF software. The basic equations used in the different CATREF modules are given in Appendix A.

[17] The following steps were followed to generate the ITRF2000 combined solution:

1. The constraints of the originally constrained solutions were removed and minimum constraints were applied, using equations (A12), (A13), and (A14). Similar approach of constraint handling is used by [*Davies and Blewitt*, 2000]. For more details about minimum constraints, see [*Sillard and Boucher*, 2001].
2. Minimum constraints were added to loosely constrained solutions, using equation (A15).
3. Solutions where analysis centers already applied minimum constraints were used as they are.
4. For each individual solution, station positions were propagated to epochs of minimal position variances (EMPV), using equations (A20), (A21), and (A22). In order to assess the relative qualities of the individual solutions used in the ITRF combination, we compute the commonly known weighted root mean scatter (WRMS) per solution based on the postfit residuals. The experience showed that the computed EMPV, at which the residuals are computed, corresponds approximately to the central epoch of observations of each station. Therefore, propagating station positions at their EMPV's ensures a more "realistic" WRMS evaluation, in positions, for each individual solution.
5. Individual solutions were analyzed, by comparisons and combinations within each technique for quality control and consistency evaluation.
6. All individual solutions together with local ties were finally combined, using the physical model described in Appendix A: equations (A9), (A10), and (A11).

[18] The last step is in fact the most critical one and includes a first run, variance factor estimation, subsequent iterations as well as outlier rejections. In the first run, a preliminary variance factor (σ_s^2, as given by equation (A16)) is estimated for each individual solution. The individual solutions are then weighted by the variance factors estimated in the first run (used as multiplicative factors of the individual variance matrices) and the combination is iterated. Inspection of postfit residuals is then performed for outlier rejections: A station is rejected if any position or velocity component exhibits a residual exceeding a certain chosen threshold. For the ITRF2000 solution it was decided to reject stations having a position or velocity normalized residual (raw residual divided by its observation a priori

error) exceeding a threshold of 4. Note that in each iteration, new individual variance factors are estimated which are then used to rescale the individual matrices for the next iteration. Outlier rejections are also operated before the next iteration. The combination is repeated until the individual variance factors as well as the variance factor of the global combination converge to unity and outlier rejections are no longer needed. This iterative process allows a refined estimation of variance factors, free from outlier influence, to the level of the chosen threshold.

[19] Five iterations were necessary to produce the final robust and refined ITRF2000 solution. The outlier rejections represent about 1% of the total data included in the ITRF2000 combination. The final estimated individual variance factors are listed in Table 1.

[20] The method used for variance component estimation described in Appendix A (section A5) shows that the more solutions included in the combination the better estimation of variance factors is obtained and the lesser number of iterations is needed. For more details concerning constraint handling and ITRF analysis strategy, see *Altamimi et al.* [2002].

4. Datum Definition

[21] From a geodetic point of view, a TRS realization through a TRF, requires 14 parameters: three translations (origin), one scale factor, three rotations (orientation) and the seven corresponding rates. Given the fact that the 14 parameters should be viewed as relative values between two TRFs, their selection should correspond to the adopted TRS definition that one wants to satisfy. However, space geodesy observations do not carry all the necessary information to completely realize a TRS. While satellite techniques are sensitive to the Earth center of mass (a natural TRF origin), VLBI is not (whose TRF origin is arbitrary defined through some constraints); the scale is dependent on the modelling of some physical parameters; and the TRF orientation (unobservable by any technique) is arbitrary or conventionally defined, through specific constraints.

[22] The Earth center of mass is the point with respect to which the orbit of dynamical techniques (LLR, SLR, GPS, DORIS) is referred. However, the center of mass is affected by various geodynamic processes of mass redistribution in the Earth interior and surface envelopes [*Barkin*, 1999], causing time variations of its position with respect to the Earth surface. In other words, the geocentric motion of the tracking stations due to this effect, is known as "geocenter motion" and likely involves periodic and secular components. Presently, most of the analysis centers do not explicitly include this effect in their models. Therefore the origin of the resulting TRF coincides in practice with the position of the center of mass averaged over the period of the used observations. In practice, the dynamical techniques have currently limited abilities to accurately measure the geocenter motion [*Ray*, 1999]. For more details on the geocenter motion and variation, see, for instance, *Watkins and Eanes* [1997], *Greff-Lefftz* [2000], *Chen et al.* [1999], and *Dong et al.* [1997].

[23] When generating a combined TRF (such as the ITRF), different options could be adopted to specify explicitly the 14 datum parameters. While the seven parameters should be selected at a given epoch, the selection of scale and translation rates depends on the significance of the relative rates of the individual TRFs included in the combination.

[24] The translation rates between satellite TRFs are heavily dependent on the network configuration, the orbit and the used observations. They may also be affected by the geocenter secular motion. The scale rate is influenced by station vertical motions and other modelling such as the troposphere, as well as technique-specific effects, such as VLBI, GPS, and DORIS antenna-related effects, and SLR station-dependent ranging biases. The orientation rate, although it could be arbitrarily chosen, should have a geophysical meaning due to tectonic plate motions.

[25] Therefore a TRS realization should take into account motions and deformations of the Earth's crust, simply because space geodesy observing sites are located on that deforming crust. Meanwhile, since space geodesy techniques make use of positions and/or motions of space objects, such as satellites and extra-galactic radio-sources in case of VLBI, consistency between Celestial Reference Frame (CRF), TRF, and EOP (connecting the two frames) should naturally be ensured for each individual (technique) TRS realization. Therefore the ITRF, being one of the three IERS global references, should be consistent with the ICRF and EOP series.

[26] Moreover, fundamental equations of Earth rotation theory are all related to a coordinate system in which any motion or deformation of the Earth does not contribute to its net angular momentum [*Munk and MacDonald*, 1973; *Kinoshita and Sasao*, 1989]. To achieve this goal, a generally accepted approach is the use of the Tisserand system of mean axes defined by minimizing the kinetic energy given by

$$T = \frac{1}{2}\int_C V^2 dm, \tag{3}$$

where dm is a mass element and V is its velocity. The most intuitive choice of the integration domain C is the Earth's crust since, as it has already been mentioned, it "carries" our geodetic observing sites and the signals of its motion and deformation are contained in the observations.

[27] One of the goals of defining a minimal kinetic energy T on the crust is to minimize its global motion that would affect the EOP. Meanwhile, deeper geodynamic processes such as mantle convection and the core–mantle boundary will still influence the Earth rotation. Minimizing T leads to null linear p and angular h momentums [see *Boucher*, 1989]:

$$p = \int_C V dm = 0 \tag{4}$$

$$h = \int_C X \times V dm = 0, \tag{5}$$

where X is the dm position vector.

[28] Equations (4) and (5) theoretically define the TRF translation and rotation rates, respectively. The scale rate, although it is not foreseen in this approach, corresponds to a physical quantity estimated by space geodesy techniques.

[29] Given the fact that satellite (dynamical) techniques estimate the geocenter motion, and so station positions are referred to the center of mass as a natural TRF origin, equation (4) is no longer needed. Meanwhile, equation (5) represents the definition of the no-net-rotation (NNR) condition over the crust.

[30] A rigorous application of equation (5) requires knowledge of the crust density as well as its thickness which may vary spatially, especially between oceans and continents. However, a difficulty occurs when one wants to evaluate the integral of equation (5). A summation is then used instead, over a certain number of observing stations or tectonic plates representing the lithosphere. Each one of these two possibilities (stations or plates) leads to a different implementation of the NNR condition.

[31] The approach of applying the NNR condition over observing stations requires careful investigation. The implied stations should satisfy minimum criteria, such as having a long enough observing period (say at least three years) and being distributed optimally over the whole Earth's surface. Moreover, the use of equation (5) in this approach needs objective selection (or delimitation) of each area element associated with each station which should take its geophysical environment into account.

4.1. Background of ITRF Datum Definition

[32] Since the ITRF94, we have started to use full variance matrices of the individual solutions incorporated in the global combination. At that time, the ITRF94 datum was achieved as follows [*Boucher et al.*, 1996]: (1) the origin (the three translation components), by a weighted mean of some SLR and GPS solutions; (2) the scale, by a weighted mean of VLBI, SLR and GPS solutions, corrected by 0.7 ppb to meet the IUGG and IAU requirement to be in TCG (geocentric coordinate time) time frame instead of TT (terrestrial time) used by the analysis centers; (3) the orientation was aligned to the ITRF92 [*Boucher et al.*, 1993]; and (4) the time evolution was ensured by aligning the ITRF94 velocity field to the model NNR-NUVEL-1A (adapted from NNR-NUVEL-1 [*Argus and Gordon*, 1991], according to *DeMets et al.* [1994]) over the seven rates of the transformation parameters.

[33] The ITRF96 was then aligned to the ITRF94, and the ITRF97 was aligned to the ITRF96 using the 14 transformation parameters [*Boucher et al.*, 1998, 1999]. Analysis of the individual solutions submitted to the ITRF2000 reveals that the ITRF97 exhibits a Z translation (and rate) with respect to most of the SLR solutions, as well as a scale factor.

[34] It then became necessary to define the ITRF2000 datum to agree with the updated space geodesy data, and it was thus decided to adopt the following datum definition:

1. The scale and its rate are defined by a weighted average of VLBI and the most consistent SLR solutions. Unlike the ITRF97 scale expressed in TCG-frame, that of the ITRF2000 is expressed in TT-frame, following the recommendations of the ITRF2000 Workshop (November 2000). This decision was adopted in order to satisfy space geodetic analysis centers contributed to ITRF2000 who use a time scale consistent with TT-frame.
2. The translations and their rates are defined by a weighted average of the most consistent SLR solutions.
3. The orientation is aligned to that of ITRF97 at epoch 1997.0 and its rate to be such that there is no-net-rotation rate with respect to NNR-NUVEL-1A. Note that the orientation as well as its rate are defined upon a selection of ITRF sites with high geodetic quality, satisfying the following criteria: (1) continuously observed during at least 3 years; (2) located on rigid parts of tectonic plates and far away from deforming zones; and (3) velocity formal error (as result of the ITRF 2000 combination) less than 3 mm/yr; and (4) velocity residuals less than 3 mm/yr for at least three different solutions;

[35] On the basis of the ITRF2000 analysis, sites selection (one point per site) was performed using the above criteria yielding 96 sites satisfying criteria 1, 3, and 4. In sites having more than one station, the priority is given to the station satisfying best criterion 3 and (if they are of the same quality) then to station with longer observation period. Note that none of the DORIS stations satisfies the above criteria. Assignment of sites to rigid tectonic plates and deforming zones was then performed with the help of D. F. Argus (following *Argus and Gordon* [1996]), providing 55 sites on rigid plates and 41 sites on deforming zones, listed in Table 2. In Table 2, sites are ordered within each plate by increasing east longitude. The 41 sites located on deforming zones were obviously not used in the orientation definition. From the 55 sites on rigid plates, only 50 sites were used, the remaining five sites being rejected for the following reasons:

1. Bahrein (Arabian plate) and Easter Island (Nazca plate) are found to have estimated ITRF2000 velocities which disagree with NNR-NUVEL-1A by about 6 and 10 mm/yr, respectively.
2. Tromso (Eurasian plate) and Flin-Flon (North American plate) show about 2 mm/yr postfit residual after NNR absolute rotation pole estimation.
3. Richmond site (United States), having more than 8 years of VLBI observations, exhibits about 15 mm position discrepancy between ITRF2000 and ITRF97 estimates due to imprecise local ties deweighted in ITRF2000 and not in ITRF97. Including this site in the core list would bias the ITRF2000/ ITRF97 orientation alignment at epoch 1997.0.

[36] Consequently, only 50 "core" sites on rigid plates were used in the ITRF2000 orientation and rate definition, shown on Figure 2.

4.2. Implementation of the ITRF2000 Datum

[37] When combining individual solutions using a physical model such as the one implemented in CATREF software and briefly described in Appendix A (equations (A9), (A10), and (A11)), the combined frame has to be defined by specifying the 14 parameters corresponding to the datum definition. Equivalently, the normal matrix, constructed by accumulating normal equations (equation (A10)-type) of the individual solutions, has a rank deficiency corresponding to the 14 transformation parameters.

[38] There are several ways to define the TRF datum in the combination model. A very simple case is to fix given values (e.g., zeros) to the 14 parameters of one solution among those included in the combination. In contrast, the implementation of the ITRF2000 datum was achieved as

Table 2. High-Quality Geodetic ITRF2000 Sites

Domes	Code[a]	Name	T[b]	Plate	λ, deg	ϕ, deg
		Sites on Rigid Plates				
31303M002	MASP	MasPalomas	P	AFRC	344.367	27.764
91201M002	KERG	Kerguelen	P	ANTA	70.256	−49.351
66010M001	DAV1	Davis	P	ANTA	77.973	−68.577
66011M001	CAS1	Casey	P	ANTA	110.520	−66.283
66001M003	MCMU	McMurdo	P	ANTA	166.669	−77.838
24901M002	BAHR	Bahrein	P	ARAB	50.608	26.209
50107M001	7090	Yarragadee	L	AUST	115.347	−29.046
50133M001	PERT	Perth	P	AUST	115.885	−31.802
50116S002	7242	Hobart	R	AUST	147.441	−42.804
50103S010	1545	Canberra	R	AUST	148.978	−35.398
13212S001	7840	Herstmonceux	L	EURA	0.336	50.867
13101M004	BRUS	Brussels	P	EURA	4.359	50.798
13504M003	KOSG	Kootwijk	P	EURA	5.810	52.178
14209S001	7203	Effelsberg	R	EURA	6.884	50.525
14001S001	7810	Zimmerwald	L	EURA	7.465	46.877
14208M001	OBER	Oberpfaffen.	P	EURA	11.280	48.086
10402S002	7213	Onsala	R	EURA	11.926	57.396
14201S004	7224	Wettzell	R	EURA	12.877	49.145
14106M003	POTS	Potsdam	P	EURA	13.066	52.379
11502M002	GOPE	Pecny	P	EURA	14.786	49.914
11001S002	7839	Graz	L	EURA	15.493	47.067
12205S001	7811	Borowiec	L	EURA	17.075	52.277
10302M003	TROM	Tromso	P	EURA	18.938	69.663
12209M001	LAMA	Lamkowko	P	EURA	20.670	53.892
10403M002	KIRU	Kiruna	P	EURA	20.968	67.857
12204M001	JOZE	Jozefoslaw	P	EURA	21.032	52.097
10503S011	METS	Metsahovi	P	EURA	24.395	60.217
12330M001	ZWEN	Zwenigorod	P	EURA	36.759	55.699
13407S010	1565	Madrid	R	EURA	355.749	40.427
13406M001	VILL	Villafranca	P	EURA	356.048	40.444
41703M003	EISL	Easter Islands	P	NAZC	250.617	−27.148
40127M003	YELL	Yellowknife	P	NOAM	245.519	62.481
40442S017	7613	Fort Davis	R	NOAM	256.053	30.637
40135M001	FLIN	Flin Flow	P	NOAM	258.022	54.726
40128M002	CHUR	Churchill	P	NOAM	265.911	58.759
40465S001	7612	North Liberty	R	NOAM	268.426	41.771
40499S001	7219	Richmond	R	NOAM	279.615	25.614
40441S001	7204	Greenbank	R	NOAM	280.164	38.438
40104S001	7282	Algonquin	R	NOAM	281.927	45.955
40451M105	7105	Washington	L	NOAM	283.172	39.021
40114M001	NRC1	Ottawa	P	NOAM	284.376	45.454
40471S001	7618	Hancock	R	NOAM	288.013	42.934
40440S003	7209	Westford	R	NOAM	288.506	42.613
43001M001	THU1	Thule	P	NOAM	291.212	76.537
42501S004	BRMU	Bermuda	P	NOAM	295.304	32.370
40101M001	STJO	St. John's	P	NOAM	307.322	47.595
43005M001	KELY	Kellyville	P	NOAM	309.055	66.987
50506M001	KWJ1	Kwajalein	P	PCFC	167.730	8.722
50207M001	CHAT	Chatham Island	P	PCFC	183.434	−43.956
40424S001	1311	Kauai	R	PCFC	200.335	22.126
40477S001	7617	Mauna Kea	R	PCFC	204.544	19.801
41510M001	LPGS	La Plata	P	SOAM	302.068	−34.907
97301M210	KOUR	Kourou	P	SOAM	307.194	5.252
41602S001	7297	Fortaleza	R	SOAM	321.574	−3.878
30602M001	ASC1	Ascension	P	SOAM	345.588	−7.951
		Deforming Zone Sites				
10002S001	7835	Grasse	L		6.921	43.755
10202M001	REYK	Reykjavik	P		338.045	64.139
12313M001	IRKT	Irkoutsk	P		104.316	52.219
12334M001	KIT3	Kitab	P		66.885	39.135
12348M001	POL2	Poligan	P		74.694	42.680
12711S001	7230	Bologna	R		11.647	44.520
12717S001	7547	Noto	R		14.989	36.876
12725M003	CAGL	Cagliari	P		8.973	39.136
12734S005	7243	Matera	R		16.704	40.650
12750M002	UPAD	Padova	P		11.878	45.407
21602M001	WUHN	Wuhan	P		114.357	30.532
21605S009	7227	Shanghai	R		121.200	31.099
21613M001	LHAS	Lhasa	P		91.104	29.657
21701S001	1856	Kashima	R		140.663	35.954
21726S001	7838	Simosato	L		135.937	33.578

Table 2. (continued)

Domes	Code[a]	Name	T[b]	Plate	λ, deg	ϕ, deg
21729S007	USUD	Usuda	P		138.362	36.133
21730S001	7311	Tsukuba	R		140.087	36.106
30302S001	7232	Hartebeest'k	R		27.685	−25.890
40105M002	DRAO	Penticton	P		240.375	49.323
40129M003	ALBH	Albert Head	P		236.513	48.390
40134M001	WILL	Williams Lake	P		237.832	52.237
40136M001	WHIT	Whitehorse	P		224.778	60.751
40400M007	JPLM	Pasadena	P		241.827	34.205
40405S009	7222	Goldstone	R		243.112	35.332
40408S002	7225	Fairbanks	R		212.502	64.978
40433M002	7109	Quincy	L		239.055	39.975
40439S002	7207	Owens Valley	R		241.717	37.231
40456S001	7234	Poetown	R		251.881	34.301
40463S001	7611	Los Alamos	R		253.754	35.775
40466S001	7610	Kitt Peak	R		248.388	31.956
40473S001	7614	Brewster	R		240.317	48.131
40489S001	7218	Hat Creek	R		238.529	40.817
40497M001	7110	Monument Peak	L		243.577	32.892
40504M001	7122	Mazatlan	L		253.541	23.343
41705S006	1404	Santiago	R		289.332	−33.151
42202M005	AREQ	Arequipa	P		288.507	−16.466
43201S001	7615	Sainte Croix	R		295.416	17.757
50127M001	COCO	Coco Islands	P		96.834	−12.188
50135M001	MAC1	Macquarie Island	P		158.936	−54.500
50209M001	AUCK	Auckland	P		174.834	−36.603
50501M002	GUAM	Guam	P		144.868	13.589

[a] Code holds for CDP (Crustal Dynamic Project) number or IGS/GPS four-character identification.
[b] IERS space geodesy technique abbreviation: R, VLBI; L, SLR; and P, GPS.

follows: (1) origin, by fixing to zero the translation and translation rate parameters between ITRF2000 and the weighted mean of the SLR solutions of five analysis centers: CGS, CRL, CSR, DGFI, and JCET; (2) scale, by fixing to zero the scale and scale rate parameters between ITRF2000 and the weighted mean of the above five SLR solutions and the VLBI solutions of the analysis centers: GIUB, GSFC, and SHA; and (3) orientation, by adding to the combination model a TRF datum equation (restricted to the orientation and its rate) given by

$$B(X_0 - X) = 0, \tag{6}$$

where (1) $B = (A^T A)^{-1} A^T$ and A is the design matrix of partial derivatives (restricted to its last three columns), as given by equation (A6) of Appendix A; (2) X_0, ITRF97

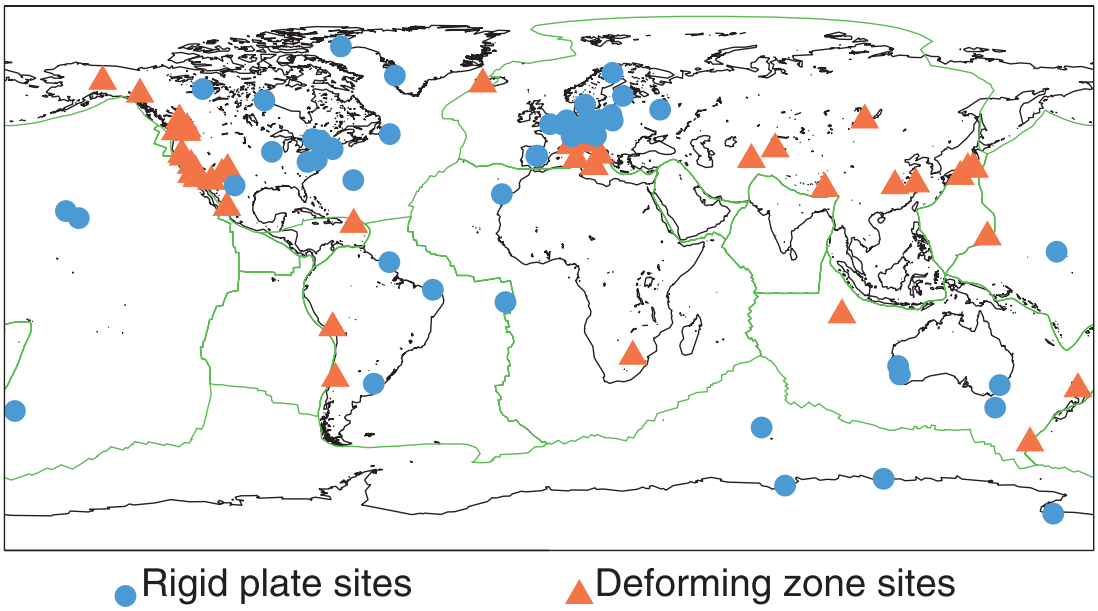

Figure 2. ITRF2000 high-quality sites. Note that only the 50 sites on rigid plates (circles) were used in the orientation rate definition of the ITRF2000 (see text).

Table 3. Transformation Parameters (at Epoch 1997.0) and Their Rates From ITRF2000 to ITRF97 and Rates to NNR-NUVEL-1A[a]

	*T*1	*T*2	*T*3	*D*	*R*1	*R*2	*R*3
			From ITRF2000 to ITRF97 (50 Stations)[b]				
	6.7	6.1	−18.5	1.55[c]	0.000	0.000	0.000
±	0.3	0.3	0.3	0.05	0.012	0.012	0.014
Rates	0.0	−0.6	−1.4	0.01	−0.001	0.004	0.019
±	0.3	0.3	0.3	0.05	0.012	0.012	0.014
			From ITRF2000 to ITRF97 (50 Stations)[d]				
	6.6	6.1	−18.5	1.55[c]	−0.003	0.001	−0.002
±	0.6	0.6	0.6	0.12	0.018	0.015	0.018
Rates	0.0	−0.6	−1.4	0.05	−0.001	0.002	0.019
±	0.6	0.6	0.6	0.09	0.015	0.015	0.015
			From ITRF2000 to NNR-NUVEL-1A (50 Stations)[b]				
Rates	0.3	0.2	0.4	−0.13	0.000	0.000	0.000
±	0.2	0.2	0.2	0.03	0.009	0.009	0.010
			From ITRF2000 to NNR-NUVEL-1A (50 Stations)[d]				
Rates	0.2	0.3	0.2	−0.11	0.001	0.000	0.002
±	0.6	0.6	0.6	0.18	0.015	0.015	0.018

[a] Units are mm for the translations and mm/yr for their rates; ppb (10^{-9}) for the scale and ppb/yr for its rate; mas for the rotations and mas/yr for their rates.
[b] Values obtained using unit weight matrix.
[c] The ITRF97 scale is expressed in the TCG frame, whereas that of the ITRF2000 is in the TT frame. The actual scale difference is then 0.85 ppb.
[d] Values obtained using a weight matrix constructed upon the inverses of the two full matrices.

positions at epoch 1997.0 defining the rotation angles and NNR-NUVEL-1A velocities defining the rotation rates; and (3) *X*, estimated station positions and velocities. It should be noted that equation (6), only applied upon the 50 selected sites, introduces six equations defining the ITRF2000 orientation (and its time evolution) and not more.

[39] The consequence of this new datum definition is that there are some significant parameter differences between the ITRF2000 and the previous ITRF97. To assess these differences as accurately as possible, 14 transformation parameters were estimated between these two frames upon the 50 core sites, yielding the values listed in Table 3. Table 3 lists also the rates of the seven transformation parameters between ITRF2000 and NNR-NUVEL-1A, also estimated upon the 50 sites.

[40] As described in Appendix A (section A2), the estimated transformation parameters between two solutions depends on the weight matrix used in this estimation. To estimate the 14 transformation parameters between ITRF2000 and ITRF97, we performed three comparisons using respectively three different options: (1) unit weights (identity matrix); (2) cumulated diagonal terms of the two inverses of the variance matrices; and (3) cumulated inverses of the two full variance matrices. The resulting values of the three sets of the 14 parameters are statically equivalent (e.g., differences are less than the formal errors, at one σ). In Table 3 we list the values of the first option (i.e., using unit weights) since it is fully consistent with the way we ensured the ITRF2000 orientation alignment to ITRF97 at epoch 1997.0, using equation (6). Meanwhile, in order to assess a statistically realistic accuracy of this alignment, Table 3 also lists the values of the third option, (i.e., using the two full matrices).

[41] Similarly, the rates of the seven transformation parameters between ITRF2000 and NNR-NUVEL-1A are listed in Table 3, following the first and third options. Since NNR-NUVEL-1A is a horizontal model, we assumed zero vertical velocity for each one of the 50 core sites. Note however that the third option consists in constructing the weight matrix upon the inverse of the full variance matrix of ITRF2000 and the inverse of a variance matrix resulting from the adoption of 3 and 10 mm/yr, respectively, for horizontal and vertical errors

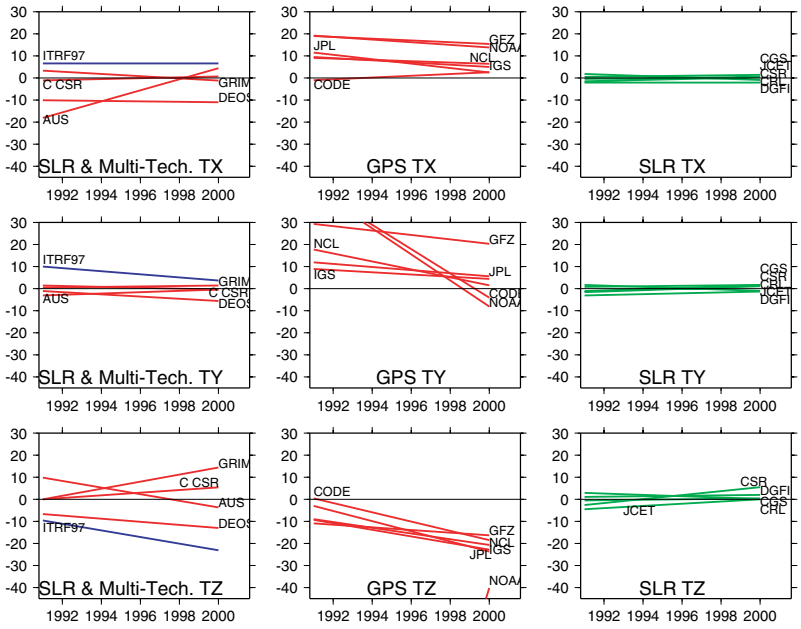

Figure 3. Translation variations (mm) of SLR, multitechnique, and GPS solutions. The third column plots show the translation variations of the five SLR solutions whose weighted average was used to define the ITRF2000 origin.

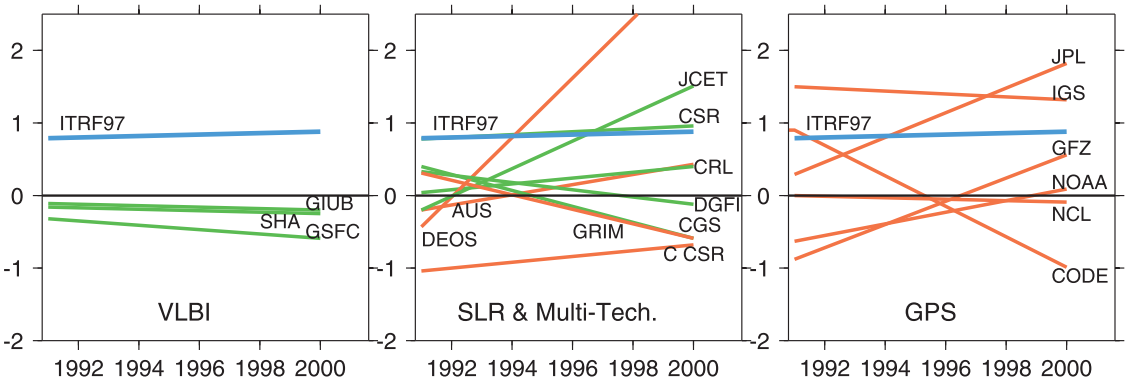

Figure 4. Scale variations (ppb) of VLBI, SLR and multitechnique, and GPS solutions. Green lines (grey in B&W version) indicate solutions whose scale weighted average was used to define the ITRF2000 scale. The ITRF97 scale, inserted on these plots, is reduced to TT frame (see text).

for NNR-NUVEL-1A velocities. The values listed in Table 3 show null rotation rates between ITRF2000 and NNR-NUVEL-1A, but small translation and scale rates which (although they are meaningless since NNR-NUVEL-1A is derived using equation (5) type, defining three rotation rate parameters) are most likely due to ITRF2000 vertical velocities for which NNR-NUVEL-1A provides no information.

[42] The two sets of the transformation parameters listed in Table 3 show no significant differences between the two estimates. This fact reflects the robustness of the selection of the 50 high-quality geodetic sites. The errors listed in Table 3 indicate that the orientation alignment of ITRF2000 to ITRF97 at epoch 1997.0 is ensured at (or better than) the 1 mm level. Similarly, the ITRF2000 orientation rate alignment to NNR-NUVEL-1A is also at the 1 mm/yr level.

5. ITRF2000 Results

[43] The results of the ITRF2000 global combination are (1) station positions at epoch 1997.0, (2) station velocities (stations within the same site are constrained to have the same velocity), (3) transformation parameters (at epoch 1997.0) and their rates between ITRF2000 and each individual frame, after removing the original constraints (if any) and applying minimum constraints, and (4) postfit residuals for each individual solution included in the global combination. Note that station positions and velocities, as well as transformation parameters are all estimated simultaneously, in a single adjustment, using the combination model described in Appendix A (section A3).

[44] Since we combine solutions with minimum constraints, we assume that the rotation parameters are uninformative. This statement is also valid for the relative origins of VLBI TRFs. Therefore we will focus on the relative scales and origins of satellite-derived solutions as well as the relative scales of VLBI solutions.

5.1. Individual TRF Origin and Scale Differences

[45] Selecting the time interval 1991–2000 as the "common" observation period of the analyzed solutions, Figure 3 shows the linear variation of the translation components for SLR and GPS solutions, relative to the ITRF2000 origin (mean of the five selected SLR solutions). Figure 4 illustrates the linear variation of the scale for VLBI, SLR, and GPS solutions, relative to the ITRF2000 scale (mean of the three VLBI and five SLR solutions). The linear variations shown in Figures 3 and 4 were computed by propagating each parameter value from epoch 1997.0 to the end point epochs (e.g., 1991.0 and 2000.0), using the relation

$$P(t) = P(1997.0) + \dot{P} \times (t - 1997.0), \qquad (7)$$

where P is a transformation parameter and $\dot{P}$ is its time derivative (rate).

[46] DORIS solutions are not represented on Figures 3 and 4, their origin differences being in the range 1–10 cm and their scale differences in the 3–8 ppb range. Note, however, that the multitechnique GRIM and CSR solutions are shown on SLR plots, since they are dominated by SLR data, especially in terms of datum definition.

[47] Figure 3 clearly shows the good agreement between the five selected SLR solutions over the three translation components, within 2 mm in X and Y and 5 mm in Z, over the whole 1991–2000 selected period. Moreover, the translation rates of the 5 SLR solutions are not significant, since they are within their uncertainties which range between 0.2 and 0.4 mm/yr in X and Y and between 0.5 and 1.0 mm/yr in Z.

[48] However, GPS solutions exhibit large discrepancies and in particular around X and Y components. Note that the translation variations of IGS, JPL, and NCL solutions follow the ITRF97, since these three centers have translated their individual solutions to the ITRF97. Note also the peculiar, unexplained large slope of CODE and NOAA solutions in the Y component, and the large Z translation of NOAA solution.

[49] Figure 4 shows the full scale agreement between the three VLBI solutions on the one hand and, on the other hand, that most of the SLR scale differences are within 1 ppb (10^{-9}). Note that the scale rates of the three VLBI solutions are completely negligible, given their uncertainty which is about 0.05 ppb/yr. On the other hand, among the 5 selected SLR solutions, three of them (CSR, CRL, and DGFI) have statistically negligible scale rates, e.g., they are within the error bare (about ±0.06 ppb/y). The scale rates of the two other solutions (CGS and JCET) are −0.11 and 0.19 (±0.06) ppb/yr, respectively. Given their opposite slopes and

Table 4. Accuracy of the ITRF2000's Origin and Scale's Datum Definition and Long-Term Stability[a]

Parameter/Rate	WRMS(1997.0)	WRMS(Over 10 years)
	Scale	
D, ppb	0.2 (≈1.2 mm)	0.5 (≈3 mm)
$\dot{D}$, ppb/yr	0.03 (≈0.2 mm/yr)	
	Origin Components	
T_x, mm	0.4	1.4
$\dot{T}_x$, mm/yr	0.1	
T_y, mm	0.5	1.5
$\dot{T}_y$, mm/yr	0.1	
T_z, mm	0.9	3.9
$\dot{T}_z$, mm/yr	0.3	

[a] Note that one ppb scale difference is equivalent to a shift of about 6 mm in station heights.

their disagreement with the three other SLR solutions, it is most likely that the vertical velocities of some stations in these two solutions are mismodeled.

[50] In order to assess the accuracy of the ITRF2000 scale and origin definition, we computed WRMS values over scale and translation differences (with respect to ITRF2000) upon the three VLBI and five SLR solutions used in the scale and origin definition. These values listed in Table 4 indicate an accuracy of the scale and origin at epoch 1997.0 at (or better than) the 1 mm level and 0.3 mm/yr for their rates.

[51] Moreover, in order to evaluate the long-term stability of the ITRF2000 scale and origin, the WRMS are propagated over 10 years and listed in Table 4. The propagated WRMS values over 10 years suggest a frame stability better than 4 mm in origin and better than 0.5 ppb in scale (equivalent to a shift of approximately 3 mm in station heights). Note however that the WRMS of the Z translation component is larger than those of X and Y. This fact is most likely due to the SLR network configuration having much more stations in the northern hemisphere.

5.2. ITRF2000 Quality Evaluation

[52] The quality of the ITRF2000 depends on the relative qualities of the contributing solutions as well as on the combination strategy equally applied to these solutions. As overall quality indicators of the individual solutions included in the ITRF2000 combination, WRMS values per technique are summarized in Table 5. The WRMS are computed over the residuals of all stations of a particular solution, using equation (A19). The WRMS values listed in Table 5 indicate that a level of 2–5 mm in positions and 1–2 mm/yr in velocities is reached by some of these solutions.

[53] It is also interesting to compare the ITRF2000 to the previous ITRF97 solution in terms of formal errors, both in positions and velocities. The formal errors are those resulting from the final global combination after the estimation of solution variance factors and weighting of solutions within the combination. They correspond to the square root of the diagonal terms of the inverse of the normal matrix of the whole combined solution (i.e., ITRF2000 estimated standard deviations). The histograms presented in Figure 5 illustrate the spherical errors computed, for each point position and velocity by the square root of the square sum of the errors of the three components. Equivalently, the spherical error corresponds to the trace of the variance of the position (respectively, velocity) vector. The significance and justification of the spherical error representation is described in Appendix A (section A7). These spherical errors were then arranged in 5 intervals for each centimeter for position errors and 5 intervals for each millimeter for velocity errors. This figure shows on the one hand an improvement of ITRF2000 compared to ITRF97 and, on the other hand, about 50% of station positions have an error less than 1 cm, and about 100 sites with velocities determined at (or better) than 1 mm/yr level.

[54] In general, it is assumed that the variance matrix associated with a given solution contains both the precision of the estimated station positions and velocities as well as the TRF datum definition effect. Therefore it is important to note that the spherical errors shown in Figure 5 reflect not only the precision of ITRF2000 station positions and velocities but also the accuracy of its datum definition, which is at the one 1 mm level.

[55] The ITRF2000 errors are more meaningful than those of ITRF97 given the fact that the individual solutions included in the ITRF2000 combination are unconstrained. The factors that reduce the ITRF2000 errors compared to ITRF97 include: minimum constraints approach equally applied to the individual solutions, outlier rejections, better use of the local ties in collocation sites (see below) and the improved quality of the individual solutions.

[56] Moreover, in order to have more insight about the significance of the ITRF2000 errors, per-technique combinations were performed whose spherical errors are shown in Figure 6. For these per-technique combinations (free from local ties), we used all the solutions included in the official ITRF2000 global combination as well as the same strategy analysis. In addition, we also estimated individual variance factors which are found to be slightly optimistic compared to those obtained from ITRF2000 combination. Variance factor differences between ITRF2000 and per-technique estimates may reach 20% (see Table 1). All the per-technique spherical errors shown in Figure 6 are those obtained from the per-technique combinations. We see clearly that they are generally more optimistic than those of the ITRF2000 combination (see, for example, VLBI position and velocity errors and GPS position errors). Reasons for such differences include local ties (for which we adopted unity variance factors, except for the dew-

Table 5. Summary of 3-D WRMS of the Individual Solutions Included in the ITRF2000 Combination

Technique	NS[a]	Position[b]		Velocity[c]	
		S[d]	L[e]	S	L
VLBI	3	2	3	1	1
LLR	1	50	50	5	5
SLR	7	2	14	1	5
GPS	6	2	5	1	2
DORIS	2	25	30	4	5
Multitechnique	2	6	9	2	2
GPS densification	9	1	8	1	4

[a] Number of solutions.
[b] Position 3-D WRMS in mm.
[c] Velocity 3-D WRMS in mm/yr.
[d] Smallest WRMS.
[e] Largest WRMS.

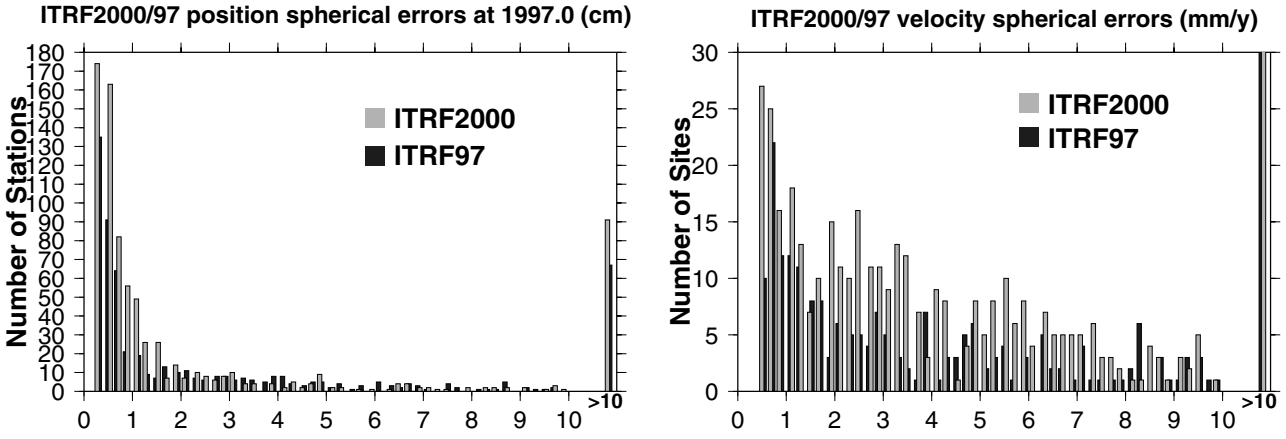

Figure 5. ITRF2000 and ITRF97 spherical errors in positions (left) at epoch 1997.0 and in velocities (right). Units are cm for positions and mm/yr for velocities. Note that position errors are for all stations, while velocity errors are for all sites since stations within the same site were constrained to have the same velocity.

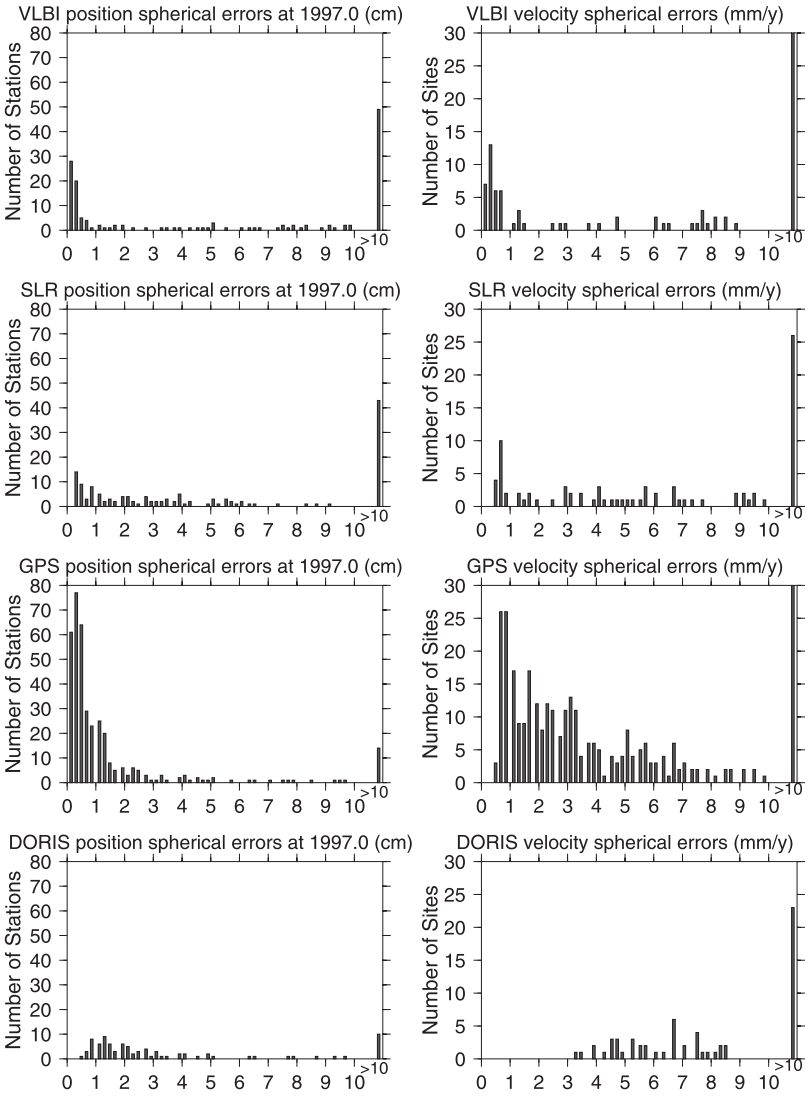

Figure 6. Spherical errors (left) in positions at epoch 1997.0 and (right) in velocities as results from per-technique combinations.

eighted ones) and possible systematic discrepancies between techniques.

5.3. ITRF2000 and Collocation Sites

[57] As illustrated in Figure 1, the ITRF2000 contains 101 sites having 2, 3 or 4 collocated techniques. Unfortunately, local ties are not all available at the time of the ITRF2000 computation. While about 200 local tie vectors were included in the combination, 38 were missing, 25 of which are highly important, given their geographic location and/or quality of their geodetic instruments. On the other hand, among the included local ties, 20 vectors are declared as dubious since their postfit residuals are larger than or equal to 1 cm. Note that ''dubious'' means either local ties or space geodesy estimates are imprecise or in error. In order to preserve the implied collocations in the combination, dubious local ties having normalized residuals exceeding the threshold of 4 were deweighted rather than rejected. Deweighting the dubious local ties consists in rescaling their standard deviations by a factor of 10, so that their normalized residuals in the final combination become less than the adopted threshold. This is for instance the case of three highly important sites where VLBI-GPS local ties disagree with space geodesy estimates. These sites are Fairbanks (Alaska), O'Higgins (Antarctica), and Westford (Massachusetts), having residuals in the vertical components, of about 2, 3, and 2 cm, respectively. In order to assess how this kind of discrepancies would affect the combination, we performed a global combination test (using all the data included in the ITRF2000) in which we assigned an error of 1 mm (instead of 6 mm used in the official ITRF2000 combination) to the VLBI-GPS local tie in Westford site. As result of this combination test, almost all VLBI and GPS coordinates are shifted in the vertical component, compared to the official ITRF2000 values, by about 1 mm for VLBI and 3 mm for GPS. The effect on the transformation parameters is found to be only in the scale factor: The relative scale factors between all VLBI and GPS solutions are affected by about 0.5 ppb. Therefore deweighting dubious local ties avoids contaminating space geodesy estimates (and so ITRF2000 results) by possible local tie errors.

6. ITRF2000 and Plate Tectonics

[58] Global relative plate motion models were derived using geological and geophysical data records, averaged over the past few million years, such as RM2 of *Minster and Jordan* [1978] and the current widely used NUVEL-1A of *DeMets et al.* [1990, 1994], dividing the lithosphere into tectonic plates (about 10 large plates and some small ones).

[59] From these relative models, absolute plate motion models were derived and referred to the fixed deep mantle assumed to be rigid or having negligible motions compared to those of tectonic plates. Two different assumptions are generally used in deriving absolute models: (1) the plates (implicitly the lithosphere) have no-net-rotation over the mantle; and (2) hot spots have no motion with respect to the mantle, or at least negligible motion as compared to those of tectonic plates. Generally, these two types of absolute models are performed by estimating the rotation pole of one plate, according to one of the two assumptions, and then deriving rotation poles of the remaining plates, using the relative models, by vector subtraction.

[60] Early absolute plate motion models were discussed by *Solomon and Sleep* [1974], followed by those of *Minster and Jordan* [1978]: AM0-2 using assumption 1 and AM1-2 using assumption 2 and the current widely used model NNR-NUVEL-1A. While relative motions of tectonic plates are clearly determined (providing motion of one plate relative to another one), absolute models are very sensitive to the underlying assumption (or TRF definition), and their differences may reach several milliarc seconds (mas) per year: the difference between AM0-2 and AM1-2 is about 1 mas/yr (3 cm/yr on the Earth surface); the velocity between NNR-NUVEL-1 and HS2-NUVEL-1 [*Gripp and Gordon*, 1990] may reach 37 mm/yr [*Argus and Gordon*, 1991].

[61] The geological NNR absolute plate motion models mentioned above are derived with a summation over assumed rigid plates using an equilibrium equation, given by *Solomon and Sleep* [1974], and easily derivable from Tisserand's equation (5) of null angular momentum. Simplifications are used in the generation of these models such as the assumption of a uniform density for all plates and neglecting their thickness variations.

[62] The alignment in orientation rate of the ITRF2000 to NNR-NUVEL-1A is then an implicit application of the NNR condition. This procedure is fully equivalent to minimizing the global rotation rate between ITRF2000 and NNR-NUVEL-1A. In addition, even if the relative model NUVEL-1A (on which the absolute model NNR-NUVEL-1A is based) has possible deficiencies, this will not disrupt the internal consistency of the ITRF2000, being insensitive to the datum definition.

6.1. ITRF2000 Velocity Field

[63] As stations within the same site were constrained to have the same velocity, ITRF2000 velocities of such sites are the average (in least squares sense) of those of individual stations available in the different solutions included in the combination. Therefore possible velocity discrepancies between solutions (or techniques) should then appear in the postfit residuals. Inspection of site velocity residuals reveals some discrepancies within and between techniques, in particular in the vertical component. As an example, in Fairbanks site (Alaska), all the GPS vertical velocity residuals are discrepant in the same direction compared to VLBI, and differences between GPS solutions may reach 5 mm/yr. Thus the velocity of this site is entirely determined by VLBI.

[64] Although the ITRF2000 orientation rate is aligned to that of NNR-NUVEL-1A, it is important to quantify the residual velocities between the two velocity fields. Figure 7 shows horizontal velocity differences between ITRF2000 and NNR-NUVEL-1A over 49 sites of the 50 selected ones (ordered as in Table 2), distributed over six plates having at least four sites. The 50th site, MasPalomas, is on the geodetically poor African plate. In Figure 7, we clearly see per-plate systematic residuals between the two velocity fields, as for example along the north–south direction: about 1.5 mm/yr for Eurasia and, in the opposite direction, about 2 mm/yr for North America. This behavior suggests a relative angular velocity difference for these two plates of approximately 3 mm/yr between ITRF2000 and NUVEL-

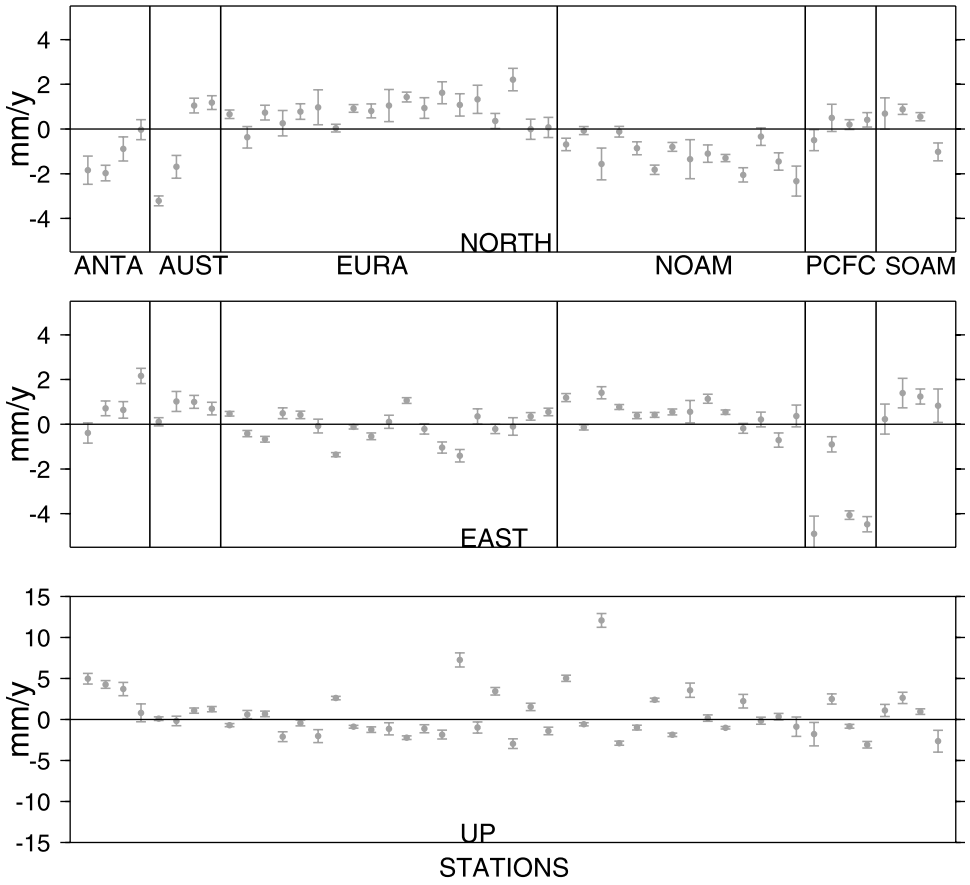

Figure 7. Velocity differences (ITRF2000 minus NNR-NUVEL-1A) in mm/yr for 49 core stations used in the orientation and rate definition. Note that UP differences are in fact vertical velocities since NNR-NUVEL-1A is a horizontal model.

1A estimates. Most importantly along the east–west component, the velocity residuals of the Pacific plate reach about 4 mm/yr for three sites. These per-plate systematic differences indicate the inadequacy of the NUVEL-1A model to describe the current plate motions as seen by the ITRF2000 results. This residual behavior also means that although we ensured the ITRF2000 alignment to NNR-NUVEL-1A, differences between the two, in terms of site velocities may exceed 3 mm/yr. Meanwhile it should be emphasized that these differences do not at all disrupt the internal consistency of the ITRF2000, simply because the alignment defines the ITRF2000 orientation rate and nothing more. The absolute rotation poles predicted by NNR-NUVEL-1A model are not equal to those which would be estimated using ITRF2000 velocities. In addition, while an ITRF2000 estimated rotation pole for a given plate depends on the sites used and the level of rigidity of that plate, NNR-NUVEL-1A always yields the same rotation pole for any sub-set of sites on that plate.

[65] In order to illustrate the discussion above, we used ITRF2000 velocities to estimate NNR absolute rotation poles for six tectonic plates, listed in Table 6. In this estimation we used the 49 sites on rigid plates listed in Table 2, augmented by O'Higgins (Antarctica plate) and Haleakala (Pacific plate) to improve the geometry and number, respectively, of sites distributed over these two plates. The linearized observation model used is based on the well-known equation linking the Euler vector ω_p with point velocity $\dot{X}_i$, of position vector X_i, located on plate p:

$$\dot{X}_i = \omega_p \times X_i. \tag{8}$$

The full variance matrix of the 51 site velocities was extracted from the ITRF2000 SINEX file and used in the Euler vectors estimation in a single inversion, thus preserving the correlations between velocity parameters. In addition, as illustrated in Figure 8, postfit velocity residuals resulting from this estimation of NNR absolute rotation poles are within ±1 mm/yr level.

6.2. ITRF2000 Relative Plate Motion Model

[66] Using the six NNR absolute rotation poles, relative poles were then derived by vector subtraction and listed in Table 7. Relative rotation poles are insensitive to the TRF orientation rate, even though the ITRF2000 velocity field is aligned to NNR-NUVEL-1A. It is then instructive to compare ITRF2000 relative poles to those predicted by NUVEL-1A, as listed in Table 7. Table 7 shows that

Table 6. ITRF2000 NNR Absolute Rotation Poles

Plate	ϕ, °N	λ, °E	ω, deg/m.y.
ANTA	61.830	−125.574	0.231
±	2.143	3.689	0.015
AUST	32.327	39.437	0.614
±	0.652	0.816	0.006
EURA	57.965	−99.374	0.260
±	1.211	2.710	0.005
NOAM	−5.036	−83.144	0.194
±	1.142	1.945	0.003
PCFC	−64.176	110.194	0.666
±	0.404	1.345	0.005
SOAM	−21.457	−134.631	0.113
±	2.806	4.762	0.005

differences between the two range between 0.03° and 0.08°/m.y., equivalent to approximately 1–7 mm/yr over the Earth's surface, at the geometric "barycenter" of each plate. As shown in Table 7, relative to the Pacific plate, we find that the angular velocities of the other plates inferred from ITRF2000 results appear to be faster than those predicted by NUVEL-1A model, except for the Australian plate. In addition, we found that the Australia and Eurasia rotation poles, relative to the Pacific plate, are located about 5 and 7°, respectively, more to the east than those predicted by NUVEL-1A model.

[67] Moreover, the ITRF2000 results show a relative motion between the two most populated plates in terms of geodetic sites, Eurasia and North America, faster than that of NUVEL-1A, by about 0.056 (±0.005) °/m.y. The location of their relative rotation pole is found to be about at 10° in latitude and 7° in longitude more to the northwest, compared to NUVEL-1A prediction.

7. Conclusions

[68] The ITRF2000 is the most extensive and accurate version of the International Terrestrial Reference Frame ever developed, containing about 800 stations located on about 500 sites. The densification part increases access to the ITRF2000 for various Earth science applications. The internal consistency of the independent SLR and VLBI solutions included in ITRF2000 allowed an accurate implementation of the global frame origin and scale at the 1 mm level. The accuracy of its long-term stability, evaluated over 10 years, is estimated to be better than 4 mm in origin and better than 0.5 ppb in scale, equivalent to a shift in station heights of approximately 3 mm over the Earth's surface. The ITRF2000's strength is that it combines space geodesy TRF solutions that are free from any external constraint, reflecting the actual precision of space geodesy techniques for station position and velocity estimates over the Earth's crust. Geophysical information inferred from this frame, such as tectonic plate motions, allows meaningful comparisons with the existing geological models, such as NUVEL-1A. Although the ITRF2000 orientation rate alignment to NNR-NUVEL-1A is ensured at the 1 mm/yr level, differences between the two may reach 3 mm/yr or more but do not alter the internal consistency of the ITRF2000. These differences are the consequence of significant disagreement between ITRF2000 and NUVEL-1A in terms of relative plate motion. This important finding indicates clearly that space geodesy techniques combined together can be used to estimate a global plate motion model (for a limited number of plates), or at least to contribute significantly to a mixed geodetic–geological model. Moreover, the densified ITRF2000 global frame provides a vast velocity field permitting detailed and localized crustal deformation evaluation in plate interiors as well as along plate boundaries. Seeking more refined datum definition in orientation rate, we finally believe that more and more thorough geodetic-based investigations have to be carried out in future to apply the NNR condition upon space geodesy observing sites which contain, unlike assumed rigid plates, more pertinent information related to the kinematic properties of the Earth's crust. The link of this condition to Earth rotation theory should also be taken into account. Finally, we believe

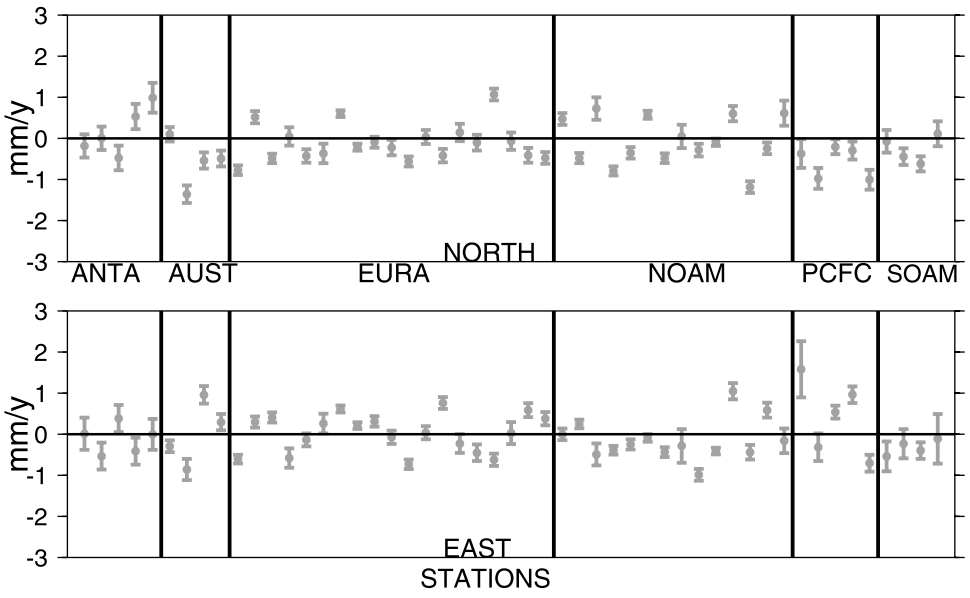

Figure 8. Postfit velocity residuals in mm/yr for 51 sites used in the estimation of ITRF2000 NNR absolute rotation poles.

Table 7. ITRF2000 Relative Rotation Poles[a]

Plate	ϕ, °N	λ, °E	Ω_x	Ω_y	Ω_z	Ω	Ω_N	$\Delta\Omega$	$\delta\Omega$
				Relative to Pacific Plate					
ANTA	65.688	−84.208	0.000640	−0.006305	0.014029	0.882	0.870	0.025	0.7
AUST	61.482	6.530	0.008747	0.001001	0.016203	1.057	1.074	0.054	4.9
EURA	63.118	−79.215	0.001357	−0.007126	0.014309	0.919	0.859	0.083	6.9
NOAM	50.488	−75.134	0.002152	−0.008107	0.010171	0.755	0.749	0.036	2.2
SOAM	−58.070	−85.633	−0.000463	0.006058	−0.009749	0.658	0.637	0.041	3.9
				Relative to North America Plate					
EURA	73.032	128.99	−0.000794	0.000981	0.004138	0.248	0.214	0.056	4.6

[a] Ω_x, Ω_y, Ω_z are the three Cartesian components of the relative rotation pole in radians/m.y. Ω and Ω_N are ITRF2000 and NUVEL-1A relative rotation pole vectors, respectively, in deg/m.y. $\Delta\Omega = |\Omega - \Omega_N|$. $\delta\Omega$ is the magnitude of velocity differences in mm/yr over the Earth's surface, at the "barycenter" of each moving plate relative to the reference one. Uncertainties are not listed but could easily be computed from Table 6.

that improvement of future ITRF solutions would not be significant without improving the local ties in the collocation sites.

Appendix A: Basic Equations for Comparison and Combination of Terrestrial Reference Frames

A1. Transformation Between Terrestrial Reference Systems

[69] The standard relation of transformation between two reference systems is a Euclidian similarity of seven parameters: three translations, one scale factor, and three rotations, designated respectively, $T1$, $T2$, $T3$, D, $R1$, $R2$, $R3$, and their first time derivatives: $\dot{T}1$, $\dot{T}2$, $\dot{T}3$, $\dot{D}$, $\dot{R}1$, $\dot{R}2$, $\dot{R}3$. The transformation of a coordinate vector X_1, expressed in a reference system (1), into a coordinate vector X_2, expressed in a reference system (2), is given by

$$X_2 = X_1 + T + DX_1 + RX_1 \tag{A1}$$

with

$$T = \begin{pmatrix} T1 \\ T2 \\ T3 \end{pmatrix} \quad R = \begin{pmatrix} 0 & -R3 & R2 \\ R3 & 0 & -R1 \\ -R2 & R1 & 0 \end{pmatrix}.$$

[70] IT is assumed that equation (A1) is linear for sets of station coordinates provided by space geodesy techniques (origin difference is about a few hundred meters, and differences in scale and orientation are of 10^{-5} level).

[71] Generally, X_1, X_2, T, D, R are functions of time. Differentiating equation (A1) with respect to time gives

$$\dot{X}_2 = \dot{X}_1 + \dot{T} + \dot{D}X_1 + D\dot{X}_1 + \dot{R}X_1 + R\dot{X}_1. \tag{A2}$$

Since D and R are of 10^{-5} level and $\dot{X}$ is about 10 cm per year, the terms $D\dot{X}_1$ and $R\dot{X}_1$ are negligible, about 0.1 mm over 100 years. Therefore equation (A2) could be written as

$$\dot{X}_2 = \dot{X}_1 + \dot{T} + \dot{D}X_1 + \dot{R}X_1. \tag{A3}$$

A2. Estimation of the Seven Transformation Parameters and Their Rates Between Two TRFs

[72] Least squares adjustment is commonly used to estimate the seven transformation parameters and their rates between two TRFs. For this purpose, equations (A1) and (A3) are rewritten as

$$X_2 = X_1 + A\theta \tag{A4}$$

$$\dot{X}_2 = \dot{X}_1 + A\dot{\theta}, \tag{A5}$$

where θ and $\dot{\theta}$ are the vectors of the seven transformation parameters and their rates, respectively. A is the design matrix of partial derivatives constructed upon approximate station positions $(\ldots, x_0^i, \ldots)$, where $1 < i < n$ and n is the number of stations:

$$A = \begin{pmatrix} . & . & . & . & . & . & . \\ 1 & 0 & 0 & x_0^i & 0 & z_0^i & -y_0^i \\ 0 & 1 & 0 & y_0^i & -z_0^i & 0 & x_0^i \\ 0 & 0 & 1 & z_0^i & y_0^i & -x_0^i & 0 \\ . & . & . & . & . & . & . \end{pmatrix}. \tag{A6}$$

[73] Least squares adjustment yields solutions for θ and $\dot{\theta}$ of equations (A4) and (A5) as follows:

$$\theta = (A^T P_x A)^{-1} A^T P_x (X_2 - X_1) \tag{A7}$$

$$\dot{\theta} = (A^T P_v A)^{-1} A^T P_v (\dot{X}_2 - \dot{X}_1). \tag{A8}$$

The estimated transformation parameters (and their rates) depend on the choice of the weight matrix P_x for station positions, and P_v for station velocities. There are mainly three choices for the weight matrix: unit weights, $P_x = I$ (respectively $P_v = I$), where I is the identity matrix; cumulated diagonal terms of the two inverses of the variance matrices associated with solutions X_1 and X_2; and cumulated inverses of the two full variance matrices.

[74] It is usually not guaranteed that the three cases will yield the same estimated values. It is, on the other hand, well known that the seven transformation parameters are correlated, particularly in the case of regional networks. Note that if the two implied TRFs are of the same quality, having global coverage, with no erroneous positions (velocities) and with well-conditioned variance matrices, the above three cases should theoretically provide the same estimated values of the transformation parameters.

[75] Note that equations (A7) and (A8) could be solved for in a single least squares adjustment in the case where the two frames contain station positions as well as velocities. In this case, the design matrix has 14 columns instead of seven given in equation (A6), the last seven columns are similar to the seven first ones, as derived from equation (A3).

A3. ITRF Combination Model

[76] A general physical model is given below, simultaneously combining station positions as well as velocities. Assuming that for each individual solution s, and each point i, we have position X_s^i at epoch t_s^i and velocity $\dot{X}_s^i$, expressed in a given TRF k.

[77] The combination consists in estimating: positions X_{itrf}^i at a given epoch t_0 and velocities $\dot{X}_{\text{itrf}}^i$, expressed in ITRS and transformation parameters T_k at an epoch t_k and their rates $\dot{T}_k$, from the ITRF to each individual frame k. The general combination physical model is given by

$$\begin{cases} X_s^i = X_{\text{itrf}}^i + \left(t_s^i - t_0\right)\dot{X}_{\text{itrf}}^i \\ \qquad + T_k + D_k X_{\text{itrf}}^i + R_k X_{\text{itrf}}^i \\ \qquad + \left(t_s^i - t_k\right)\left[\dot{T}_k + \dot{D}_k X_{\text{itrf}}^i + \dot{R}_k X_{\text{itrf}}^i\right] \\ \\ \dot{X}_s^i = \dot{X}_{\text{itrf}}^i + \dot{T}_k + \dot{D}_k X_{\text{itrf}}^i + \dot{R}_k X_{\text{itrf}}^i \end{cases} \tag{A9}$$

where for each individual frame k, D_k, T_k, and R_k are respectively the scale factor, the translation vector and the rotation matrix.

[78] The combination model given in equation (A9) provides for each individual solution s the following normal equation:

$$\begin{pmatrix} A1_s^T \\ \\ A2_s^T \end{pmatrix} P_s \left(A1_s \quad A2_s\right) \begin{pmatrix} X \\ \\ T_k \end{pmatrix} = \begin{pmatrix} A1_s^T P_s B_s \\ \\ A2_s^T P_s B_s \end{pmatrix}, \tag{10}$$

where $A1_s$ and $A2_s$ are design matrices defined (for each point i) by

$$A1_s^i = \begin{pmatrix} I & dt_s^i I \\ \\ 0 & I \end{pmatrix}, \quad A2_s^i = \begin{pmatrix} A_s^i & dt_k^i A_s^i \\ \\ 0 & A_s^i \end{pmatrix} \tag{A11}$$

with $dt_s^i = t_s^i - t_0$, $dt_k^i = t_s^i - t_k$, and A_s^i is the design matrix relative to point i as defined by equation (A6). P_s is the weight matrix (the inverse of the variance matrix of solution s) and B_s is the vector of (Observed−Computed) parameters, in terms of least squares adjustment. The unknown parameters in equation (A10) are X: station positions & velocities and T_k: transformation parameters from ITRF to frame k.

A4. Constraint Handling

[79] In the case where constraints are introduced in an estimated solution X_s^{est}, containing station positions and velocities, the selected method of combination is to remove them by subtracting the inverse of the estimated (Σ_s^{est}) and constraint (Σ_s^{const}) matrices:

$$\left(\Sigma_s^{\text{unc}}\right)^{-1} = \left(\Sigma_s^{\text{est}}\right)^{-1} - \left(\Sigma_s^{\text{const}}\right)^{-1}. \tag{A12}$$

Note that it is most likely that the resulting unconstrained matrix $(\Sigma_s^{\text{unc}})^{-1}$ is singular due to the fact that it has a rank deficiency corresponding to some of the TRF datum parameters among the 14 ones (three translations, one scale factor, three rotations; and their corresponding rates). To complete this rank deficiency, minimum constraints are then added to obtain the minimally constrained variance matrix Σ_s^{mc}:

$$\left(\Sigma_s^{\text{mc}}\right)^{-1} = \left(\Sigma_s^{\text{unc}}\right)^{-1} + \left(B^T \Sigma_\theta^{-1} B\right), \tag{A13}$$

where $B = (A^T A)^{-1} A^T$ is the matrix containing all the information necessary to define the TRF datum, depending on the shape of the implied network. Note that B is made up of appropriate columns of A given in equation (A6). Σ_θ is a diagonal matrix containing small variances for the 14 transformation parameters. The resulting deconstrained solution ($\overline{X}_s$) then becomes

$$\overline{X}_s = \Sigma_s^{\text{mc}} \left[\left(\Sigma_s^{\text{est}}\right)^{-1} X_s^{\text{est}} - \left(\Sigma_s^{\text{const}}\right)^{-1} X_s^{\text{const}}\right], \tag{A14}$$

where X_s^{const} is the a priori parameter vector with which constraints were applied.

[80] In the case of a loosely constrained solution (e.g., in which some station positions and velocities are constrained to a priori values with $\sigma \geq 1$ m for positions and ≥ 10 cm/yr for velocities), the corresponding variance matrix is augmented by minimum constraints in order to define the TRF datum using:

$$\Sigma_s^{\text{mc}} = \Sigma_s^{\text{est}} - \Sigma_s^{\text{est}} B^T \left(B \Sigma_s^{\text{est}} B^T + \Sigma_\theta\right)^{-1} B \Sigma_s^{\text{est}}. \tag{A15}$$

A5. Variance Component Estimation and RMS

[81] When combining solutions of station positions and velocities coming from heterogeneous sources, it is therefore postulated that each individual variance matrix is known to a given scale factor (or variance factor: σ_s). This latter is computed iteratively through a variance components estimation technique.

[82] Designating by v_s the vector of position and velocity postfit residuals of solution s, the variance factor is computed by

$$\sigma_s^2 = \frac{v_s^T P_s v_s}{f_s}. \tag{A16}$$

As seen in equation (A16), f_s is the generalization of the redundancy factor appearing in the classical estimate of the variance factor (χ^2) of a least squares adjustment. That is why we define f_s as the redundancy factor given by

$$f_s = 6n_s - \text{tr}\left(A_s \nu A_s^T P_s\right) \tag{A17}$$

with n_s number of stations of solution s; ν inverse of the normal matrix of the whole combined solution; A_s design matrix of partial derivatives of solution s; P_s weight matrix of solution s: ($P_s = \Sigma_s^{-1}$). A similar procedure of variance component estimation is used by *Davies and Blewitt* [2000].

[83] The usual RMS estimator is computed using

$$\mathrm{RMS}_s = \sqrt{\frac{{v_s^X}^T v_s^X}{f_s^X}}, \tag{A18}$$

where v_s^X is the vector of residuals restricted to station positions, and f_s^X is the redundancy factor computed over station positions, estimated as in equation (A17).

[84] The weighted RMS (WRMS) is computed by

$$\mathrm{WRMS}_s = \sqrt{\frac{{v_s^X}^T D\left(\Sigma_s^X\right)^{-1} v_s^X}{\frac{\mathrm{tr}\left(D\left(\Sigma_s^X\right)^{-1}\right)}{3n_s} \times f_s^X}} \tag{A19}$$

with $D(\Sigma_s^X)$ being a diagonal matrix extracted from the original individual variance matrix, related to the station positions part. Velocity RMS and WRMS estimators are also derived in a similar way as equations (A18) and (A19).

A6. Epoch of Minimal Position Variance

[85] For a given station with position vector X at epoch t_s and velocity vector $\dot{X}$, the variance propagation law gives its variance at epoch t as

$$\mathrm{Var}(X(t)) = \mathrm{Var}(X(t_s)) + 2(t - t_s)\,\mathrm{Cov}\left(X, \dot{X}\right) + (t - t_s)^2 \mathrm{Var}\left(\dot{X}\right). \tag{A20}$$

The epoch of minimal position variance t is the epoch which minimizes the variance of the station position so that:

$$\frac{d[\mathrm{tr}(\mathrm{Var}(X(t)))]}{dt} = 0. \tag{A21}$$

Note that we minimize the *trace* of the variance computed over the 3 components (x, y, z) of the position vector X, taking into account its velocity components ($\dot{x}$, $\dot{y}$, $\dot{z}$), so that

$$t = t_s - \frac{[\mathrm{Cov}(x, \dot{x}) + \mathrm{Cov}(y, \dot{y}) + \mathrm{Cov}(z, \dot{z})]}{[\mathrm{Var}(\dot{x}) + \mathrm{Var}(\dot{y}) + \mathrm{Var}(\dot{z})].} \tag{A22}$$

A7. Spherical Error

[86] Let X_i be the vector of Cartesian coordinates of point i at a given epoch, and Σ_i the associated covariance matrix. There exists a local frame in which Σ_i becomes diagonal. Let P being the rotation matrix that defines the frame transformation. By construction, $P\Sigma_i P^T$ is a diagonal matrix and is actually the variance of the vector U_i defined by ($\mathbb{E}$ is the expectancy)

$$U_i = P(X_i - \mathbb{E}(X_i)) = \begin{pmatrix} u_i^1 \\ u_i^2 \\ u_i^3 \end{pmatrix}.$$

The components u_i^j of U_i are random variables which can be interpreted as error terms over the three coordinates of the rotated vector PX_i. Let us consider the norm of the ith point error vector: $\Delta_i = \sqrt{{u_i^1}^2 + {u_i^2}^2 + {u_i^3}^2}$. One can see that $\mathbb{E}(\Delta_i^2) = \mathrm{tr}(P\Sigma_i P^T) = \mathrm{tr}(\Sigma_i)$ and, finally, the spherical error defined by

$$\delta_i = \sqrt{\mathbb{E}(\Delta_i^2)} = \sqrt{\mathrm{tr}(\Sigma_i)}$$

can be interpreted as the square root of the second moment of the random variable Δ_i (i.e., $\delta_i = \sqrt{\mathrm{Var}(\Delta_i) + [\mathbb{E}(\Delta_i)]^2}$).

[87] Thus the spherical error δ_i measures the dispersion (in the distance sense) of the error vector $X_i - \mathbb{E}(X_i)$ around the true position $\mathbb{E}(X_i)$ of the ith point.

[88] **Acknowledgments.** The ITRF activities are funded by the Institut Géographique National (IGN France), hosting the IERS ITRS Product Center, and partly by the Groupe de Recherches de Géodésie Spatiale (GRGS). We are indebted to all IERS analysis centers who constantly provide data for ITRF solutions which would not exist without their valuable contributions. Analysis centers listed in Table 1 are particularly acknowledged here for their significant effort in providing unconstrained solutions for this special ITRF2000 release. Fruitful discussions within the ITRF Working Group members (too numerous to be cited here) have been found very helpful. We are particularly grateful to all the institutions who provide the necessary budgets for the space geodesy observatories, which constitute the main ITRF foundation. We acknowledge useful critics and suggestions provided by two anonymous reviewers which improved the content of this article.

References

Altamimi, Z., C. Boucher, and L. Duhem, The worldwide centimetric terrestrial reference frame and its associated velocity field, *Adv. Space Res.*, *13*(11), 151–160, 1993.

Altamimi, Z., C. Boucher, and P. Sillard, New trends for the realization of the International Terrestrial Reference System, *Adv. Space Res.*,*30*(2), 175–184, 2002.

Argus, D. F., and R. G. Gordon, No-net-rotation model of current plate velocities incorporating plate motion model NUVEL-1, *Geophys. Res. Lett.*, *18*, 2038–2042, 1991.

Argus, D. F., and R. G. Gordon, Tests of the rigid-plate hypothesis and bounds on intraplate deformation using geodetic data from very long baseline interferometry, *J. Geophys. Res.*, *101*, 13,555–13,572, 1996.

Barkin, Y. V., Secular effects in the motion of the Earth's center of masses, in *IERS Analysis Campaign to Investigate Motions of the Geocenter*, edited by J. Ray, *IERS Tech. Note 25*, pp. 3–13, Obs. de Paris, Paris, 1999.

Blewitt, G., Y. Bock, and J. Kouba, Constraining the IGS polyhedron by distributed processing, in *Densification of ITRF Through Regional GPS Networks*, edited by J. F. Zumberge and R. Liu, pp. 21–37, IGS Cent. Bur., Jet Propul. Lab., Pasadena, Calif., 1994.

Boucher, C., Current intercomparisons between CTS's, in *Reference Frames in Astronomy and Geophysics*, edited by J. Kovalevsky, I. I. Mueller, and B. Kolaczek, Kluwer Acad., Norwell, Mass., 1989.

Boucher, C., Terrestrial coordinate systems and frames, in *Encyclopedia of Astronomy and Astrophysics*, Version 1.0, pp. 3289–3292, Inst. of Phys. Publ., Bristol, UK, 2000.

Boucher, C., and Z. Altamimi, Towards an improved realization of the BIH terrestrial frame, *The MERIT/COTES Report on Earth Rotation and Reference Frames*, vol. 2, edited by I. I. Mueller, pp. 551–564, Ohio State Univ., Dep. of Geol. Sci., Columbus, 1985.

Boucher, C., and Z. Altamimi, Development of a conventional terrestrial reference frame, in *Contributions of Space Geodesy to Geodynamics: Earth Dynamics*, *Geodyn. Ser.*, vol. 24, edited by D. E. Smith and D. L. Turcotte, pp. 89–97, AGU, Washington, D. C., 1993.

Boucher, C., and Z. Altamimi, International Terrestrial Reference Frame, *GPS World*, *7*, 71–74, 1996.

Boucher, C., Z. Altamimi, and L. Duhem, ITRF92 and its associated velocity field, *IERS Tech. Note15*, Obs. de Paris, Paris, 1993.

Boucher, C., Z. Altamimi, M. Feissel, and P. Sillard, Results and analysis of the ITRF94, *IERS Tech. Note20*, Obs. de Paris, Paris, 1996.

Boucher, C., Z. Altamimi, and P. Sillard, Results and analysis of the ITRF96, *IERS Tech. Note24*, Obs. de Paris, Paris, 1998.

Boucher, C., Z. Altamimi, and P. Sillard, The 1997 International Terrestrial Reference Frame (ITRF97), *IERS Tech. Note27*, Obs. de Paris, Paris, 1999.

Chen, J. L., C. R. Wilson, R. J. Eanes, and R. S. Nerem, Geophysical interpretation of observed geocenter variations, *J. Geophys. Res.*, *104*, 2683–2690, 1999.

Davies, P., and G. Blewitt, Methodology for global geodetic time series estimation: A new tool for geodynamics, *J. Geophys. Res.*, *105*, 11,083–11,100, 2000.

DeMets, C., R. G. Gordon, D. F. Argus, and S. Stein, Current plate motions, *Geophys. J. Int.*, *101*, 425–478, 1990.

DeMets, C., R. G. Gordon, D. F. Argus, and S. Stein, Effect of recent revisions of the geomagnetic reversal timescale on estimates of current plate motions, *Geophys. Res. Lett.*, *21*, 2191–2194, 1994.

Dong, D., J. O. Dickey, Y. Chao, and M. K. Cheng, Geocenter variations caused by atmosphere, ocean and surface ground water, *Geophys. Res. Lett.*, *24*, 1867–1870, 1997.

Geodesist's Handbook, *Bull. God.*, *66*, 128 pp., 1992.

Greff-lefftz, M., Secular variation of the geocenter, *J. Geophys. Res.*, *105*, 25,685–25,692, 2000.

Gripp, A. E., and R. G. Gordon, Current plate velocities relative to the hotspots incorporating the NUVEL-1 global plate motion model, *Geophys. Res. Lett.*, *17*, 1109–1112, 1990.

Kinoshita, H., and T. Sasao, Theoretical aspects of the Earth rotation, in *Reference Frames in Astronomy and Geophysics*, edited by J. Kovalevsky, I. I. Mueller, and B. Kolaczek, pp. 173–211, Kluwer Acad., Norwell, Mass., 1989.

Kovalevsky, J., I. I. Mueller, and B. Kolaczek (Eds.), *Reference Frames in Astronomy and Geophysics*, 474 pp., Kluwer Acad., Norwell, Mass., 1989.

McCarthy, D., (Ed.), *IERS Standards*, *IERS Tech. Note 13*, Obs. de Paris, Paris, 1992.

McCarthy, D., (Ed.), *IERS Conventions*, *IERS Tech. Note 21*, Obs. de Paris, Paris, 1996.

Minster, J. B., and T. H. Jordan, Present-day plate motions, *J. Geophys. Res.*, *83*, 5331–5354, 1978.

Munk, W. H., and G. J. F. Macdonald, *The Rotation of the Earth: A Geophysical Discussion*, 323 pp., Cambridge Univ. Press, New York, 1973.

Observatoire de Paris, BIH annual reports for 1985, Paris, 1986.

Observatoire de Paris, BIH annual reports for 1986, Paris, 1987.

Observatoire de Paris, BIH annual reports for 1987, Paris, 1988.

Petit, G., Report of the BIPM/IAU Joint Committee on relativity for space-time reference systems and metrology, in *Proceedings of IAU Colloquium 180*, edited by K. J. Johnston et al., pp. 275–282, U.S. Nav. Obs., Washington, D. C., 2000.

Ray, J., (Ed.), IERS analysis campaign to investigate motions of the geocenter, *IERS Tech. Note 25*, 121 pp., Obs. de Paris, Paris, 1999.

Sillard, P., and C. Boucher, Review of algebraic constraints in terrestrial reference frame datum definition, *J. Geod.*, *75*, 63–73, 2001.

Sillard, P., Z. Altamimi, and C. Boucher, The ITRF96 realization and its associated Velocity field, *Geophys. Res. Lett.*, *25*, 3223–3226, 1998.

Solomon, S. C., and N. H. Sleep, Some simple physical models for absolute plate motions, *J. Geophys. Res.*, *79*, 2557–2567, 1974.

Watkins, M. M., and R. J. Eanes, Observations of tidally coherent variations in the geocenter, *Geophys. Res. Lett.*, *24*, 2231–2234, 1997.

Wilkins, G. A., Review of the achievements of project MERIT for the intercomparison of techniques for monitoring the rotation of the Earth, in *The Earth's Rotation and Reference Frames for Geodesy and Geodynamics*, *Proc. IAU Symp.*, vol. 128, edited by A. K. Babcock and G. A. Wilkins, pp. 227–232, Kluwer Acad., Norwell, Mass., 1989.

Z. Altamimi and P. Sillard, Institut Géographique National, ENSG/LAREG, 6–8 Avenue Blaise Pascal, F-77455 Marne-la-Vallée, France. (altamimi@ensg.ign.fr; sillard@ensg.ign.fr)

C. Boucher, Ministère de la Recherche, Département Espace et Aéronautique, 1 rue Descartes, F-75231 Paris, France. (claude.boucher@ign.fr)